Proceedings of ICMM2003
Microchannels and Minichannels
April 24-25, 2003, Rochester, New York, USA

ICMM2003-1104

INK JET PROCESSING OF METALLIC NANOPARTICLE SUSPENSIONS FOR ELECTRONIC CIRCUITRY FABRICATION

John B. Szczech[1], Constantine M. Megaridis[1], Jie Zhang[2], and Daniel Gamota[2]

[1]Department of Mechanical and Industrial Engineering, University of Illinois at Chicago, Chicago, IL 60607, USA
E-mails: jszcze1@uic.edu, cmm@uic.edu

[2]Motorola Labs, Schaumburg, IL 60196, USA
E-mails: gamota@motorola.com, jie.zhang@motorola.com

ABSTRACT

A novel approach in creating circuit electrodes with features as fine as 100 μm is demonstrated using a single 38 μm diameter orifice, piezoelectrically driven print head to deposit metallic nanoparticle suspensions. The suspensions consist of gold particles of ~20 nm diameter suspended in toluene solvent. The amount of gold nanoparticles present in the suspension is 30% wt. Inductor and capacitor electrode patterns are deposited onto a glass substrate and thermally processed at 300°C for 15 minutes to drive off the solvent and allow the nanoparticles to sinter, thereby yielding a conductive path with a resistivity of $O(10^{-7})$ Ω m.

INTRODUCTION

Over the years, ink jet printing has been used to print a variety of materials other than traditional pigmented inks used in photo imaging. Recently, commercial ink jet manufacturers such as Hewlett-Packard and Seiko Epson are investigating ink jet as a means to print organic polymers to manufacture flexible, low cost electronic displays (Economist, 2002). Researchers have been using ink jet systems to print several types of novel materials such as metallo-organic solutions (Vest and Singaram, 1989), molten metals (Baggerman and Schwarzbach, 1998; Wallace and Hayes, 1997), ceramic suspensions (Reis and Derby, 2000), light emitting polymers (Bharathan and Yang, 1994; Hebner et al., 1998) and metallic nanoparticle suspensions (Szczech et al., 2002; Fuller et al., 2002).

Ink jet printing is normally performed by a droplet generator or print head. Most print heads today operate by the drop-on-demand (DOD) principle, in which droplets are generated only when required. A DOD print head primarily consists of a small cavity having two end openings. One opening leads to an orifice where fluid passes through to form droplets, while the other end leads to a constant supply of fluid. In order to create droplets, a pressure impulse is generated inside the cavity by either a (1) vapor bubble which is created by suddenly heating the fluid in the cavity with a heating element, or (2) sudden movement of the cavity walls by means of a piezoelectric (PZT) crystal (Antohe and Wallace, 2002; Feng, 2002). If the pressure impulse provides the fluid with enough momentum to overcome the surface tension restoring forces at the orifice, a droplet will form.

Using DOD ink jet technology to manufacture circuitry offers many benefits. Since the technology is data driven, rapid prototyping and design changes can be implemented by modifying a graphics or data file, which, in turn, instructs the ink jet system when and where the droplets need to be generated. In addition, the printing process is additive, which reduces the number of processing steps, as well as chemical waste, which is often associated with subtractive fabrication methods such as substrate etching.

In order to fabricate electronic components, such as capacitors or inductors, conducting metallization or electrode layers are required to allow the flow of electrons. To produce such layers with ink jet technology requires a material that is not only printable but also conductive, once it has been printed. In addition, the surface of the electrode should be smooth to facilitate the printing of successive layers of metallization or other electronic materials, such as dielectric polymers or organic semi-conductors. The electrodes can be fabricated by printing molten metals or metallo-organic solutions, but today oxidation, rough surface finishes and limited electrical conductivity are prevalent. The jetting of molten gold would be ideal, however, the melting point of bulk gold is 1064°C (CRC

Handbook: 82nd Ed., 2002) which far exceeds the operating temperatures of commercially available DOD ink jet systems.

Fortunately, thermodynamic studies investigating the melting temperature of gold as a function of particle size, performed by Buffat and Borel (1976), have shown that as the particle size approaches 2.5 nm the melting point is approximately 330°C, as shown in Fig. 1. This is due to the high surface area to volume ratio the nanoparticles possess, which makes nearby particles form bonds readily even at moderate temperatures. Today, specialized material companies manufacture homogeneous, gold nanoparticle suspensions that have suitable fluid properties for use with DOD ink jet print heads. However, the print head optimal tuning conditions must be determined in order to successfully print such materials.

In this paper, we demonstrate the use of a PZT driven DOD printing device, at frequency f = 155 Hz, to dispense a gold nanoparticle suspension and fabricate gold electrode layers for use in capacitor and inductor manufacturing.

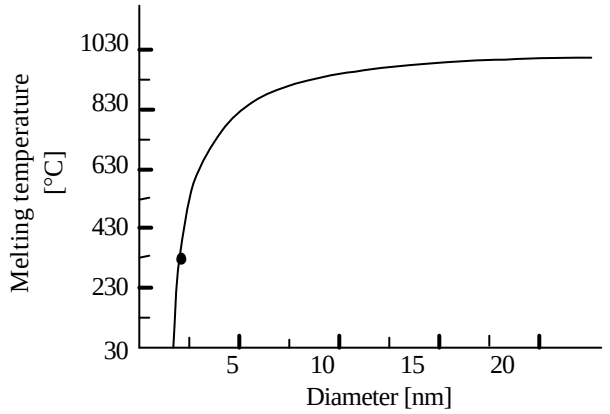

Fig. 1 Melting temperature of gold nanoparticles as a function of particle diameter. The plot is a reproduction of the chart reported by Buffat and Borel (1976).

EXPERIMENTAL TECHNIQUES

Print head

To demonstrate the ability of using ink jet technology to create electrode layers, a PZT driven DOD print head device, shown in Fig. 2, was used in conjunction with a gold nanoparticle suspension. The print head device is a capillary glass tube measuring 3.36 cm in length, with an outside diameter of 700 μm and a wall thickness of about 100 μm. At the ejection end of the tube, the inner diameter of the tube tapers over a distance of 1 mm until it converges to form an orifice of 38 μm in diameter. The other end of the capillary tube is connected to a reservoir that provides a constant fluid supply. bonded to the glass tube is a radially polarized, PZT crystal that is 1.5 cm long with an outside diameter of 1.3 mm.

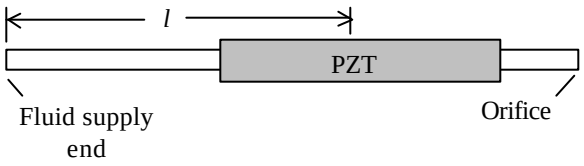

Fig. 2 Sketch of the print head device used in the study. The dark tube is the annular, radially polarized PZT crystal that is bonded to the glass capillary tube. The length *l* is the distance of the midpoint of the piezoelectric crystal to the fluid supply end of the capillary tube. For the print head used in this paper, *l* = 21.9 mm.

PZT excitation signal

To actuate the PZT crystal, the bipolar voltage signal depicted in Fig. 3 is used. According to Chen and Basaran (2002), the waveform pattern used to excite the PZT crystal dramatically affects the droplet formation process. A common voltage waveform pattern used to activate PZT driven DOD printing devices is the single, square voltage pulse. However, using a single voltage pulse signal causes the creation of unwanted secondary droplets and asymmetric droplet formations, which skew the droplet trajectory, thus missing the designated impact site on the substrate. Bipolar voltage signals minimize these occurrences and cause the droplet formations to be axisymmetric, thereby, increasing the accuracy of droplet placement. However, the additional signal parameters associated with bipolar signals further complicate the optimal tuning of the print head.

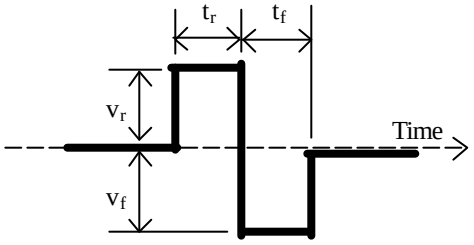

Fig. 3 Sketch of the excitation signal used to activate the PZT crystal. The subscripts *r* and *f* are used to describe the rise and fall portions of the signal, respectively. The terms *v* and *t*, respectively represent the voltage amplitude and dwell period of the signal. Each parameter of the signal can be changed independently. The frequency of the signal can be varied as well.

The rise portion of the excitation signal causes the PZT crystal to radially expand, whereas the fall portion of the signal causes the crystal to radially contract. Together these movements generate negative and positive pressure pulses in the capillary tube, resulting in the ejection of droplets (Bogy and Talke, 1984). A sequence of images depicting a

droplet evolving from the droplet present generator orifice is shown in Fig. 4.

When fabricating electronic circuits using DOD ink jet techniques, it is crucial that only one droplet is formed when needed and that its trajectory is correct to ensure accurate placement. Otherwise, circuit shorts or opens will exist. To achieve these conditions the print head must be optimally tuned. Tuning of the print head is performed by varying the excitation voltage signal until a single droplet, with a maximum obtainable velocity, is formed by the device. DOD ink jet performance evaluations performed by Wallace (1989) have shown that the droplet velocity reaches a maximum with variations in the rise pulse dwell. Antohe and Wallace (2002) described the optimal rise dwell value as the time it takes a pressure wave to travel from its point of origin to the supply end and back to its origin. They provided the following relation

$$t_{opt} = 2l'/c \qquad (1)$$

The term l' in equation (1) represents the corrected length from the midpoint of the piezoelectric crystal to the fluid supply end of the capillary tube due to end effects, and is defined as

$$l' = l + 0.61r \qquad (2)$$

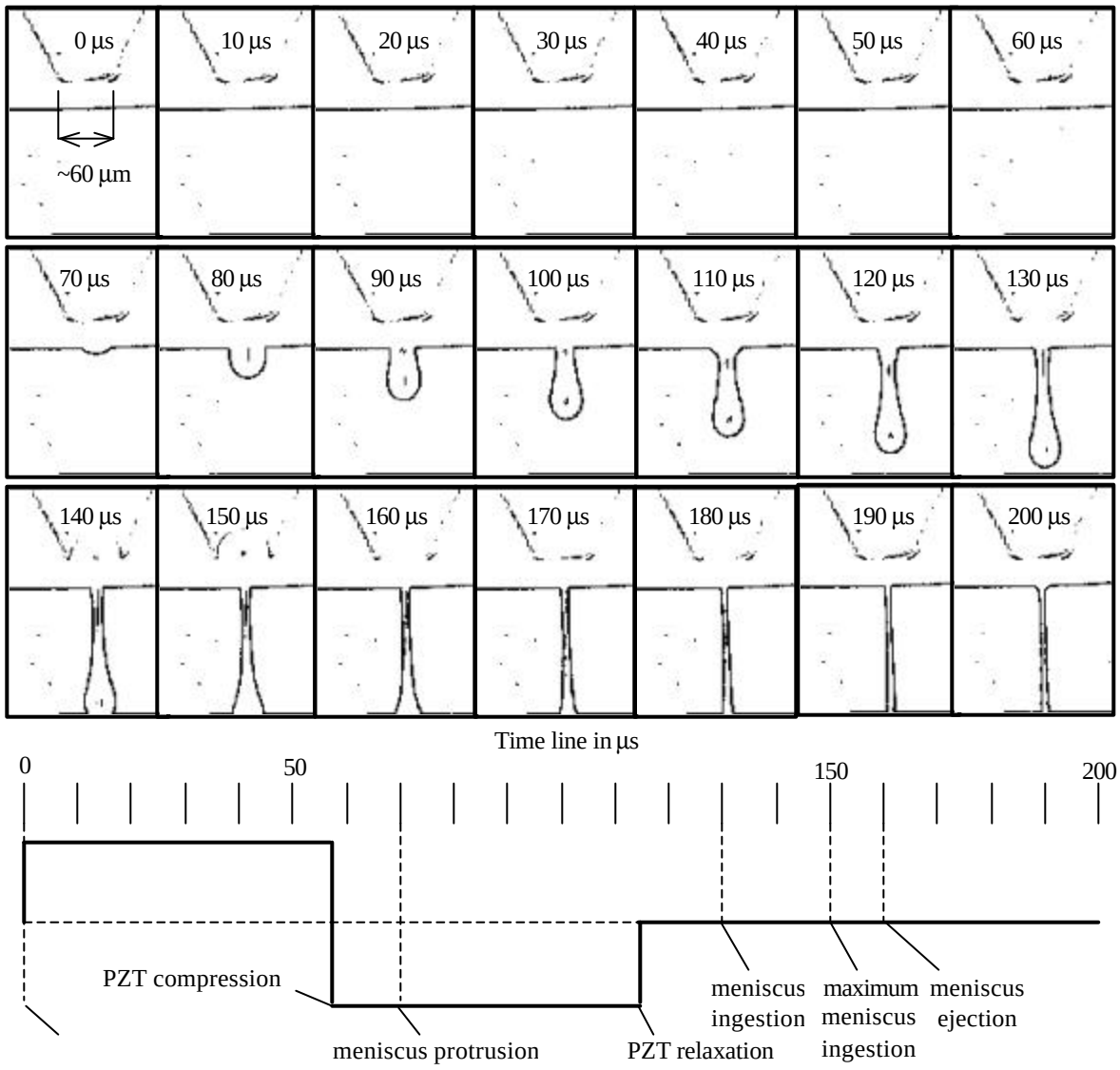

Fig. 4 Sequence of images obtained from flash photography at 10 µs increments showing the successive stages of droplet formation. The fluid shown in the images is a silicon oil with a viscosity of μ = 10 mPa s and surface tension of σ = 21 mN/m. Time proceeds from left to right and top to bottom. The images were altered to accent only the surface edges. Below the images is a time line that represents the excitation signal and the corresponding response of the fluid.

where r is the inner radius of the capillary tube diameter. The term c in equation (1) is the effective speed at which sound travels through the fluid occupying the capillary tube cavity. It is given by

$$c = \frac{c_o}{\sqrt{1 + Bg}} \tag{3}$$

The term g signifies the compliance of the capillary tube and is the relative change of the tube cross sectional area when a unitary pressure is applied on the inner walls of the tube. The term c_o is the speed of sound as an intrinsic property of the fluid, and B is the bulk modulus of elasticity of the fluid. B can be calculated from the fluid density r and c_o

$$B = rc_o \tag{4}$$

The speed at which sound travels through toluene was determined by Pal and Sharma (1998) to be c_0 = 1306 m/s. Once the optimal rise dwell is known, the remaining voltage signal parameters are adjusted until a single droplet is obtained.

Nanoparticle suspension

One of the difficulties to using DOD inkjet technology for electrode fabrication is the stringent requirement of the conductive ink's physicochemical properties (Croucher and Hair, 1989). Most commercially available conductive inks possess too high viscosity and surface tension to allow droplet formations of O(10 μm) size. However, developments in nanoparticle suspension technology have created a new category of low viscosity conductive inks suitable for use with DOD. The particular material used in this study consists of gold nanoparticles ~20 nm in diameter.

The nanoparticles are suspended in a toluene based solvent that acts to separate the particles, thereby creating a near homogeneous dispersion. In addition to toluene, other metals, such as copper, are included in the suspension to improve adherence to the substrate. Typical physicochemical properties of the gold suspension at 25°C are: μ = 1.5 mPa s, σ = 28 mN/m, and ρ = 1.35 g/cm^3. The properties may be altered by the addition or removal of toluene. Unfortunately, due to the rapid evaporation rate of toluene, the properties of the suspension vary dramatically over time and can change from a low viscosity liquid to a viscoelastic body in a matter of a few seconds upon exposure to ambient conditions. This phenomenon adversely affects jetting performance, since it can create a membrane at the orifice during droplet ejection and effectively clog the printing device. Therefore, to understand the tuning characteristics of the print head, pure toluene solvent was used to observe droplet formation optimization as a result of varying excitation signal parameters.

RESULTS AND DISCUSSION

As a starting point, an optimal dwell rise was calculated by assuming $c = c_o$ in equation (1). This gave a value of t_{opt} = 35 μs. The rise dwell of the signal was set to this value and the fall dwell of the signal was set to 800 μs to aid in dampening meniscus oscillations. The frequency was set to 155 Hz and the voltage amplitudes v_r and v_f were increased equally until stable drop formation occurred. Once stable drop formation was obtained, the rise dwell was varied from 0.1 to 300 μs and the corresponding droplet velocities recorded. The rise dwell was then set to the dwell time that produced the highest droplet velocity. The voltage amplitudes were again adjusted equally until the print head produced droplet formations that generated only one drop per excitation. The rise dwell was again varied and the corresponding droplet velocities recorded. This procedure was also repeated with a print head having an orifice diameter of 60 μm and having identical geometric dimensions compared to the 38 μm orifice print head. The velocities were plotted against the rise dwell values and produced the bell shaped curves shown in Fig. 5.

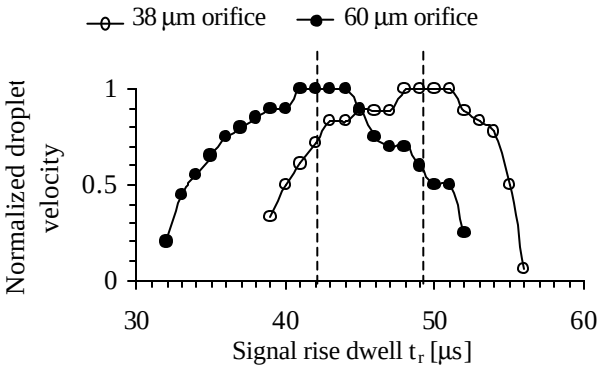

Fig. 5 Plot of the normalized droplet velocities as a function of rise dwell variation for two printing devices having different orifice diameters but identical geometric dimensions.

According to the curves seen in Fig. 5, the optimal rise dwell for the 38 μm and 60 μm orifice print heads were, 49.5 μs and 42.5 μs, respectively. However, according to equation (1) the optimal rise dwell should be identical for both print heads regardless of the orifice diameter. The possible source for the discrepancy may be in the way the walls of the PZT crystal of each print head moved. Ideally, both PZT crystals should expand and contract symmetrically about their central axis. However, since both crystals are not carbon copies of each other, as a result of variances during manufacturing, it is quite possible that movement of the crystal walls is asymmetrical, therefore causing a difference between the two optimal rise dwell values.

Another interesting phenomenon that was observed during the tuning of the print heads was the ingestion of air

bubbles into the capillary tube (Fig. 6) by the meniscus. As a result, the droplet formation ceased and resumed only when the cavity was purged with pressurized toluene solvent. Therefore, optimal tuning of the print head is critical for successful and continuous droplet formations.

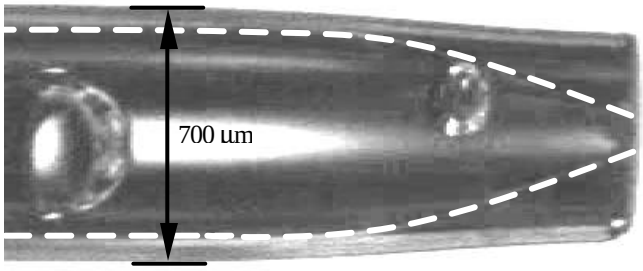

Fig. 6 Optical image of the glass capillary tube tip showing bubbles formed in toluene. These bubbles attached to the inner capillary wall as a result of air ingestion by the meniscus during an untuned printing condition. The overlaid dashed lines outline the inner surface of the tube. The 38 µm orifice is located at the far right of the tube.

After the optimal rise dwell for toluene was determined, the print head was purged of the solvent and the nanoparticle suspension fluid was loaded in its place. The nanoparticle suspension was then patterned onto a glass substrate to fabricate gold electrodes for capacitor, see Fig. 7, and inductor, see Fig. 8, circuits. The glass substrate and electrode layers where then thermally processed at 300°C for 15 minutes. An optical profilometer was used to measure the average surface roughness (6 nm) and thickness (0.6 µm). The conductivity of the electrodes was measured using a four probe multimeter. The resistivity of the gold electrodes was measured to be $O(10^{-7})$ Ω m.

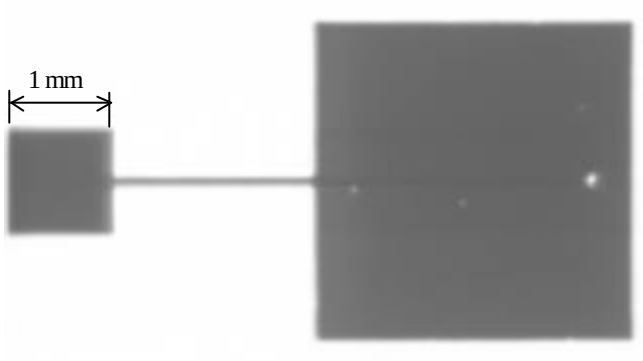

Fig. 7 Optical image of the printed gold capacitor electrode on a glass substrate after thermal processing. The structure was created by printing a single layer of the gold nanoparticle suspension.

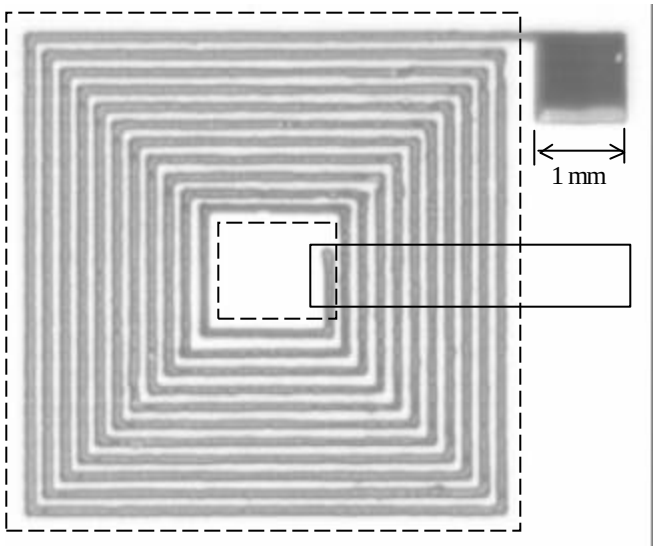

Fig. 8 Optical image of the printed gold inductor electrode after thermal processing. A single layer of gold nanoparticle suspension was printed to create the structure. The region between the two drawn dashed boxes is reserved for a dielectric material. The drawn, solid lined rectangle indicates where the next gold electrode is to be printed once the dielectric layer is in place.

CONCLUSION

Gold electrodes were created using a single, PZT driven DOD printing device having an orifice diameter of 38 µm to deposit a gold nanoparticle suspension containing ~20 nm gold particles onto a glass substrate. The signal amplitude voltages used to create the structures were $v_r = -v_f = 12$V and corresponding dwell times used were $t_r = 18$ µs and $t_f = 800$ µs. A 30% wt concentration of gold was used and a 3-axis computer controlled stage was used to move the print head to regions where droplet placement was desired. After the gold was deposited, the glass substrate was thermally processed for 15 minutes at 300°C to drive off the suspension solvent and to allow the gold particles to sinter. The fabricated gold electrodes had had an average surface roughness and thickness of 6 nm and 0.6 mm, respectively. The measured resistivity was $O(10^{-7})$ Ω m. As a comparison, the electrical resistivity for pure gold and copper at 20°C are 3.5×10^{-10} Ω m and 2.8×10^{-11} Ω m, respectively (CRC Handbook: 82nd Ed., 2002).

Continuing efforts are being made to fabricate capacitors and inductors using only DOD ink jet printing as the manufacturing process. Recently, a high temperature, liquid polyamide dielectric has been identified for use with the fabricated gold electrodes. Preliminary trials have shown that polyamide dielectric withstands the thermal process used to sinter the gold nanoparticles. With such encouraging results it seems that the fabrication of all ink jet printed, robust and functional passive electronic circuits is possible.

NOMENCLATURE

B = bulk modulus elasticity of a fluid [Pa]
c_0 = speed of sound as intrinsic property of a fluid [m/s]
c = effective speed of sound in the tube cavity [m/s]
l = length from the midpoint of the piezoelectric crystal to the fluid supply end of the capillary tube [m]; Fig. 2.
l' = corrected length from the midpoint of the piezoelectric crystal to the fluid supply end of the capillary tube [m]; Eq (2).
r = inner radius of the capillary tube [m]
t = time [s]
t_r = signal rise dwell time [s]
t_{opt} = optimal signal rise dwell time [s]
t_f = signal fall dwell time [s]
v = voltage [V]
v_r = signal rise voltage amplitude [V]
v_f = signal fall voltage amplitude [V]
g = compliance of the capillary tube [Pa^{-1}]
μ = dynamic fluid viscosity [kg/m s^2]
ρ = fluid density [kg/m^3]
σ = surface tension [kg/s^2]

REFERENCES

Antohe, B. V., and Wallace, D. B., 2002, Acoustic Phenomena in a Demand Mode Piezoelectric Ink jet Printer, *Journal of Imaging Science and Technology*, vol. 46, no. 5, pp. 409-414.

Baggerman, A. F. J. and Schwarzbach, D., 1998, Solder-Jetted Eutectic PbSn Bumps for Flip-Chip, *IEEE Transactions on Components, Packaging and Manufacturing Technology – Part B*, vol. 21, no. 4, pp. 371-381.

Bharathan, J. and Yang, Y., 1994, Polymer Electroluminescent Devices Processed by InkJet Printing: I. Polymer Light-Emitting Logo, *Applied Physics Letters*, vol. 72, no. 21, pp. 2660-2662.

Bogy, D. B. and Talke, F. E., 1984, Experimental and Theoretical Study of Wave Propagation Phenomena in Drop-On-Demand Ink Jet Devices, *IBM Journal of Research and Development*, vol. 28, no. 3, pp. 314-321.

Buffat, P., and Borel, J. P. , 1976, Size Effect on the Melting Temperature of Gold Particles, *Physical Review A*, vol. 13, no. 6, pp. 2287-2298.

Chen, A. U., and Basaran, O. A., 2002, A New Method for Significantly Reducing Drop Radius without Reducing Nozzle Radius in Drop-On-Demand Drop Production, *Physics of Fluids*, vol. 14, no. 1, pp. L1-L4.

CRC, Handbook of Chemistry and Physics, 2001/02, 82nd edition, ed. D. Lide, Cleveland, OH: CRC Press, p. 4-132.

Croucher, M. D., and Hair, M. L., 1989, Design Criteria and Future Directions in Ink Jet Ink Technology," *Ind. Eng. Chem. Res.*, vol. 28, no. 11, pp. 1712-1718.

Economist, 2002, Move Over, Silicon, December 14 issue, pp. 20-21.

Feng, J. Q., 2002, A General Fluid Dynamic Analysis of Drop Ejection in Drop-on-Demand Ink Jet Devices, *Journal of Imaging Science and Technology*, vol. 46, no. 5, pp. 398-408.

Fuller, S. B., Wilhelm, E. J., and Jacobson, J. M., 2002, Ink-Jet Printed Nanoparticle Microelectromechanical Systems, *Journal or Microelectromechanical Systems*, vol. 11, no. 1, pp. 54-60.

Hebner, T. R., Wu, C. C., Marcy, D., Lu, M. H., and Sturm, J. C., 1998, Ink-Jet Printing of Doped Polymers for Organic Light Emitting Devices, *Applied Physics Letters*, vol. 72, no. 5, pp. 519-521.

Pal, A., and Sharma, S., 1998, Speed of Sound and Isentropic Compressibilities of 2-[2-(2-alkoxyethoxy)-ethoxy]ethonal plus Toluene at the Temperature 298.15K, *Indian Journal of Pure and Applied Physics*, vol. 36, no. 8, pp. 428-433.

Reis, N., and Derby, B., 2000, Ink Jet Deposition of Ceramic Suspensions: Modelling and Experiments on Droplet Formation, *Symposium Proceedings. Materials Development for Direct Write Technologies*, vol. 624, pp. 65-70.

Szczech, J. B., Megaridis, C. M., Gamota, D. R., and Zhang, J., 2002, Fine-Line Conductor Manufacturing Using Advanced Drop-On-Demand PZT Printing Technology, *IEEE Transactions on Electronics Packaging Manufacturing*, vol. 25, no. 1, pp. 26-33.

Vest, R. W., and Singaram, S., 1989, Silver Ink for Jet Printing, *NASA Tech Brief*, vol. 13, no. 8, pp. i,1-2.

Wallace, D. B., and Hayes, D. J., 1998, Solder Jet Technology Update, *The International Journal of Microcircuits and Electronic Packaging*, vol.21, no. 1, pp. 1-4.

Wallace, D. B., 1989, A Method of Characteristics Model of a Drop-on-Demand Ink-Jet Device Using an Integral Method Drop Formation Model, *ASME Publication*, 89-WA/FE-4, pp. 1-9.